Impact Factor (SJIF): 6.092 E-ISSN: 2583-1615

International Journal of Research in Academic World

Received: 14/July/2024 IJRAW: 2024; 3(8):193-199 Accepted: 21/August/2024

# The Impact of Contamination of Groundwater Using Electrical Resistivity Method: A Case Study of Palar River, Ambur

*[1]Vangala Satish Kumar and [2]Alwal Narsing Rao

*[1]Research Scholar, Department of Environmental Sciences, Osmania University, Telangana, India.

[2]Retired Professor, Department of Environmental Sciences, Osmania University, Telangana, India.

**Abstract**

In the present study the effluent discharged from tanneries industries along the Palar River was investigated using an integrated electrical resistivity approach. A of 19 Vertical Electrical Soundings (VES) and 32 Electrical Resistivity Tomography (ERT) were conducted within the study area to delineate subsurface geology and to map the effluent plume. All vertical electrical sounding (VES) and 6 electrical resistivity tomography profiles were considered in the study area. The electrical soundings were carried out with total spreading of 100 and 200 meters whereas 120 to 240 meters was carried for electrical resistivity tomograph. Electrode configuration includes Schlumberger and Wenner array for Sounding and Tomography. The current scenario of pollution was established using parameters such as Longitudinal Conductance (Si), aquifer vulnerability index and overburden protective capacity derived from the VES analysis. The four principal geoelectric layers inferred from the VES data include the topsoil, sand, sandy clay and hard rock. Resistivity values for these layers vary from 4.9 to 310, 4.5 to 659, 4.2 to 1030, and 91.5 to 9000 Ωm with a corresponding thickness of 0.4-8.9, 1.03-24.7, 2.1-33 and 5-24.9 m respectively. The effluent plume occurs to a maximum depth of approx. 15 meters in the 2-D inverse models. The correlation between longitudinal conductance and overburden protective capacity show that aquifer in study area have moderate to good protective capacity and moderate to highly vulnerable to contamination. The pervious topsoil, sand and sandy layers increased the aquifers vulnerable to contamination by failing to act as an efficient barrier against seepage.

**Keywords:** Contamination vulnerability, resistivity tomography, vertical electrical soundings, protective capacity, longitudinal conductance, aquifers

## Introduction

The leather industry in India represents the fourth largest export sector, contributing significantly to economic growth and employment, particularly within Tamil Nadu. This state concentrates approximately 60% of the nation's tanneries [1], with clusters of these facilities located in towns along the Palar River, a important water body in the region. Notably, Ambur, Gudiyattam, Vaniyambadi, and Ranipet collectively host 76 tanneries, highlighting the industry's regional importance. Despite its economic benefits, the leather industry raises considerable environmental sustainability concerns due to the extensive use of tanning materials such as chromium and other inorganic chemicals. These substances exhibit high mobility and have been documented to negatively impact surrounding ecosystems [2]. Research specifies that the pollution footprint of a single tannery can extend over a radius of 7 to 8 kilometers, worsening environmental impacts and posing significant risks to groundwater quality [3]. Geophysical methods have emerged as valuable tools for evaluating groundwater quality and contamination risks. Among these methods, resistivity techniques, particularly Vertical Electrical Sounding (VES), have gained prominence due to their simplicity in instrumentation, ease of field deployment, and straightforward data interpretation compared to alternative techniques [4, 5]. VES techniques have demonstrated efficacy in evaluating groundwater quality across diverse lithological settings. Their advantages include the simplicity of instrumentation, ease of field logistics, and straightforward data analysis [6, 4, 7, 5]. Additionally, VES surveys are effective in studying groundwater conditions, assessing subsurface geoelectrical layers, and determining the thickness and depth of water-bearing formations [8, 9, 10, 11].

The resistivity of geological structures varies significantly, influenced by factors such as porosity, water content, and groundwater salinity. Water resistivity, for example, can range from 0.2 to over 100 Ω-m depending on ionic concentration and dissolved solids content [12]. Similarly, the resistivity of natural water and sediments without clay can vary from 1 to 120 Ω-m [13]. Consequently, geoelectric resistivity surveys alone may not adequately distinguish between lithological and groundwater quality effects [14]. To enhance the effectiveness of VES surveys, it is essential to

*Corresponding Author: Vangala Satish Kumar

correlate them with in-situ groundwater chemistry data obtained through sample collection. This integration enables a comprehensive understanding of the lateral and vertical extent of tannery contamination and its implications for groundwater quality and environmental sustainability. To delineate the lateral and vertical extent of tannery contamination comprehensively, geophysical investigations, including 2D electrical imaging coupled with chemical analysis of groundwater, are invaluable [15]. These methods provide a multidimensional view of subsurface conditions, allowing for precise mapping of contamination plumes and their spatial distribution. Combining geophysical techniques enhances the efficacy of contaminant detection and migration tracking. This integrated approach facilitates the formulation of robust long-term remediation plans aimed at mitigating the adverse impacts of tannery contamination on groundwater resources and environmental sustainability. The objective of this study is to utilize geophysical methods, specifically Vertical Electrical Sounding and 2D electrical imaging, for interpreting effluent seepage without the need for geochemical analysis sampling.

**Location and Geology of Study Area**

The study area extents approximately 39 km$^2$ along the banks of the Palar River, situated roughly 190 km west of Chennai city, Tamil Nadu, India. Positioned within latitudes North Lat. 12°45'30"-12°49'20" and East Long. 78°40'50"-78°44'35", it falls within Survey of India Toposheet 57-L/9 & 13 (Fig 1). The presence of a cluster of tanneries spanning both sides of the river, with Ambur emerging as a focal point renowned as the "Leather City." Ambur's tanneries specialize in the production of footwear for globally recognized brands, while also hosting manufacturing units of Indian companies [16, 17]. However, the area is polluted due to tannery effluent discharge, rendering groundwater unsuitable for consumption. Geologically, the study area exhibits a distinction formation: Archaean-age crystalline rocks and Quaternary alluvial deposits. The alluvial deposits are prominent along the course of the Palar River, characterized by sand, gravel, and sandy clay, with thicknesses increasing towards the eastern direction. In contrast, the south-eastern region is dominated by charnockite formations, while gneiss formations predominate in the north-western sector. These geological formations have undergone extensive metamorphic processes, resulting in the development of gneissic rock formations (Fig 2). Additionally, secondary geological structures such as joints, fractures, as well as intrusions of dolerite dykes and quartz veins, further characterize the geological landscape of the area.

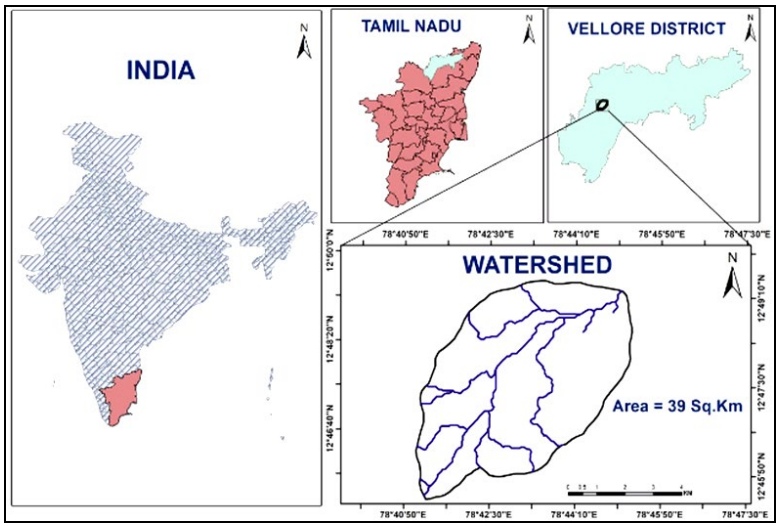


**Fig 1:** Location Map

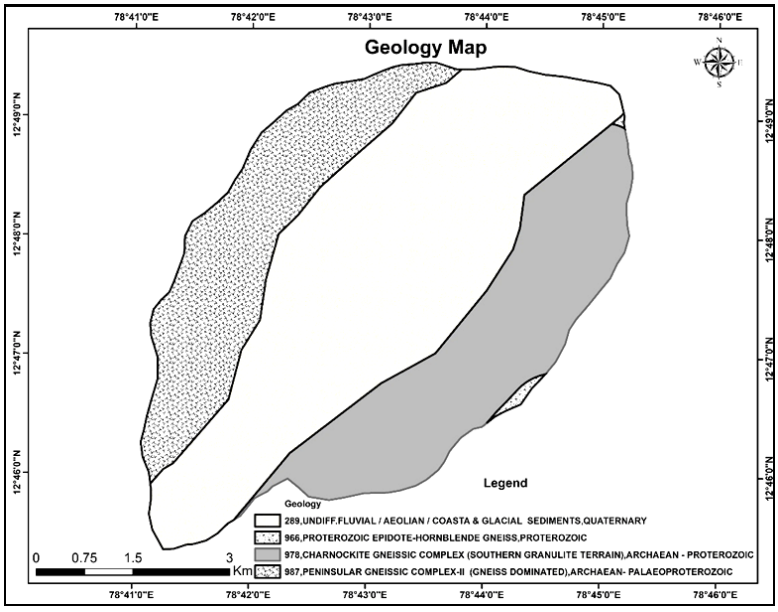


**Fig 2:** Geology Map

## Methodology

Geophysical investigations, such as vertical electrical soundings (VES) and multielectrode resistivity imaging (MERI) surveys, were conducted to decipher sub-surface geology and delineate structural features and contaminated zones [18, 19, 20]. Combining the sounding and profiling data provides a detailed picture of the sub-surface through two-dimensional (2D) cross-sections [21]. A total of 19 VESs were performed in the study area (Fig. 3) using the [22] configuration, utilizing the indigenous DDR-2 Resistivity Meter (NGRI make, Hyderabad) with a maximum current electrode spacing of 120 m. The field data were interpreted using a conventional partial curve matching technique [23] with two-layer master curves and auxiliary diagrams [24].

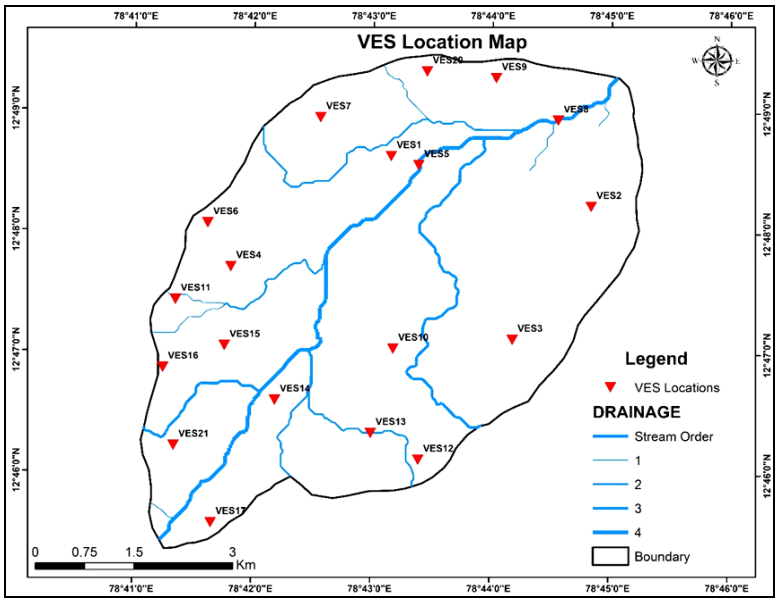


**Fig 3:** VES Location Map

The interpreted layer parameters were then used as initial estimates for inverse interpretation based on optimization techniques, employing the RESIST version 1.0 software [25]. The sub-surface layered parameters were interpreted as ρ1, ρ2, and ρ3, which are the true resistivities of the first, second, and third layers, respectively. Correspondingly, h1, h2, and h3 represent the thicknesses of these layers. The apparent resistivity values were used to calculate parameters such as the aquifer vulnerability index (AVI) and overburden protective capacity [26]. The protective capacity of groundwater aquifers is a function of the covering layers, usually referred to as the protective layers [27]. Surface water percolates through these protective layers, leading to groundwater recharge. During this percolation process, contaminant degradation can occur through mechanical, physicochemical, and microbiological processes. Effective groundwater protection is provided by protective layers with sufficient thickness and low hydraulic conductivity, resulting in a high residence time of percolating water. The aquifer vulnerability index (AVI) quantifies aquifer vulnerability by hydraulic resistance, which is a function of the thickness and hydraulic conductivity of each protective layer to vertical water flow. Typical values for hydraulic conductivity were based on [28, 26] subsequently classified aquifers with high hydraulic resistance as having low vulnerability to contamination. Furthermore, the overburden protective capacity in the area was evaluated using longitudinal unit conductance (Si) derived from the first-order parameters obtained from the VES results as in (Table 1) [29, 30].

$S_i$ is a second-order geoelectric parameter calculated using the Eq. (1)

$$S_i = \sum_{i=1}^{n} hi/\rho i$$

$\rho_i$ is the layer resistivity, $h_i$ is the layer thickness for the $i^{th}$ layer.

In this investigation, SYSCAL Junior Switch (IRIS make, France) resistivity equipment was used, with a maximum of 24 and 48 electrodes at a 5 m unit electrode spacing. The collected data were interpreted using a finite difference code developed by [31] and modified by [32], available as the software package RES2DMOD. This package was used to decipher aquifer geometry and the vertical and horizontal variation of electrical conductivity within the study area (Fig. 4). Thus, these geophysical investigations, specifically VES and MERI surveys, were meticulously conducted to comprehensively understand sub-surface geology and delineate structural features and contaminated zones within the study area. The integration of VES and MERI data facilitated the generation of detailed 2D cross-sections, providing an intricate depiction of the sub-surface structure and contaminant distribution [21].

**Table 1:** Longitudinal unit conductance ($S_i$)

| Long | Lat | Soundings | $S_i$ |
|---|---|---|---|
| 78.71875 | 12.80967 | VES1 | 3.26664 |
| 78.7412 | 12.79922 | VES2 | 1.928795 |
| 78.73795 | 12.78612 | VES3 | 3.134375 |
| 78.69768 | 12.7954 | VES4 | 1.681826 |
| 78.72315 | 12.80922 | VES5 | 2.383902 |
| 78.6937 | 12.80107 | VES6 | 1.080082 |
| 78.70614 | 12.81498 | VES7 | 0.343399 |
| 78.74263 | 12.81553 | VES8 | 5.819762 |
| 78.73392 | 12.82133 | VES9 | 2.873485 |
| 78.7211 | 12.82748 | VES10 | 1.028846 |
| 78.68873 | 12.78896 | VES11 | 0.41685 |
| 78.72335 | 12.76854 | VES12 | 0.275835 |
| 78.71668 | 12.77218 | VES13 | 0.255548 |
| 78.70323 | 12.77667 | VES14 | 3.766553 |
| 78.69613 | 12.78415 | VES15 | 1.616667 |
| 78.68753 | 12.78107 | VES16 | 0.913491 |
| 78.69358 | 12.75943 | VES17 | 0.404907 |
| 78.72339 | 12.82347 | VES20 | 1.183732 |
| 78.69109 | 12.7695 | VES21 | 0.433773 |

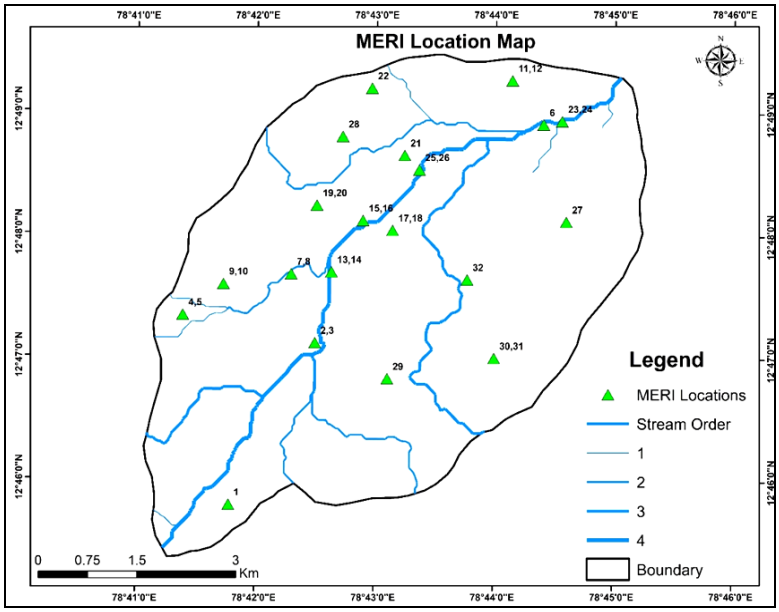


**Fig 4:** MERI Profile Map

## Results and Discussion

The results from VES sounding shows that the topsoil is characterized at shallow depth by zone of High resistivity values suggestive of the presence of a Dry Sandy type Soil. Hence, we interpret the low resistivity anomaly as areas of contamination. Due to the presence of the ion concentration the effluent normally has low resistivity values [33]. In the present study, the contamination has resistivity of 2-5 Ω m while for electrical sounding, the resistivity of the contamination is 4.5 Ω m (Fig.5). The resistivity of the contamination in this work is in accordance with the result obtained by previous workers such as [34] 1-10 Ω m and [35] < 6 Ω m. Consequently, the low resistivity values could have been attributed to even Sandy-clay in the topsoil. However, the top soil in the study area is generally of coarse sand. An important observation is that the lowest resistivity values were estimated around the river course when compared to the rest of the area.

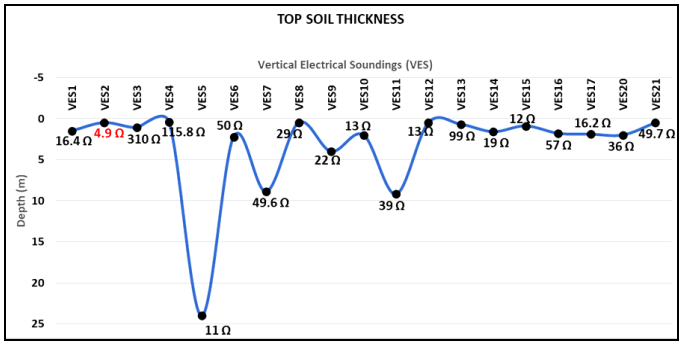


**Fig 5:** Soil Thickness Profile

The results from the 2D resistivity imaging, a total of 6 2D imaging was taking into consideration all along the palar river it states that the subsurface is having a very low resistivity values from a depth of 3-16 meters as in the (Fig. 6a, 6b & 6c). The imaging states that the contamination is migrating from the stream towards the east and west direction i.e. both sides of the river. Due to the sandy tops soil, there is scope to infiltrate into soli at the faster rate and there after it tends to move as per the subsurface which has been observed in this 2D imaging. The categorizes of this contamination is done by the [36] in (Table 2 & 3).

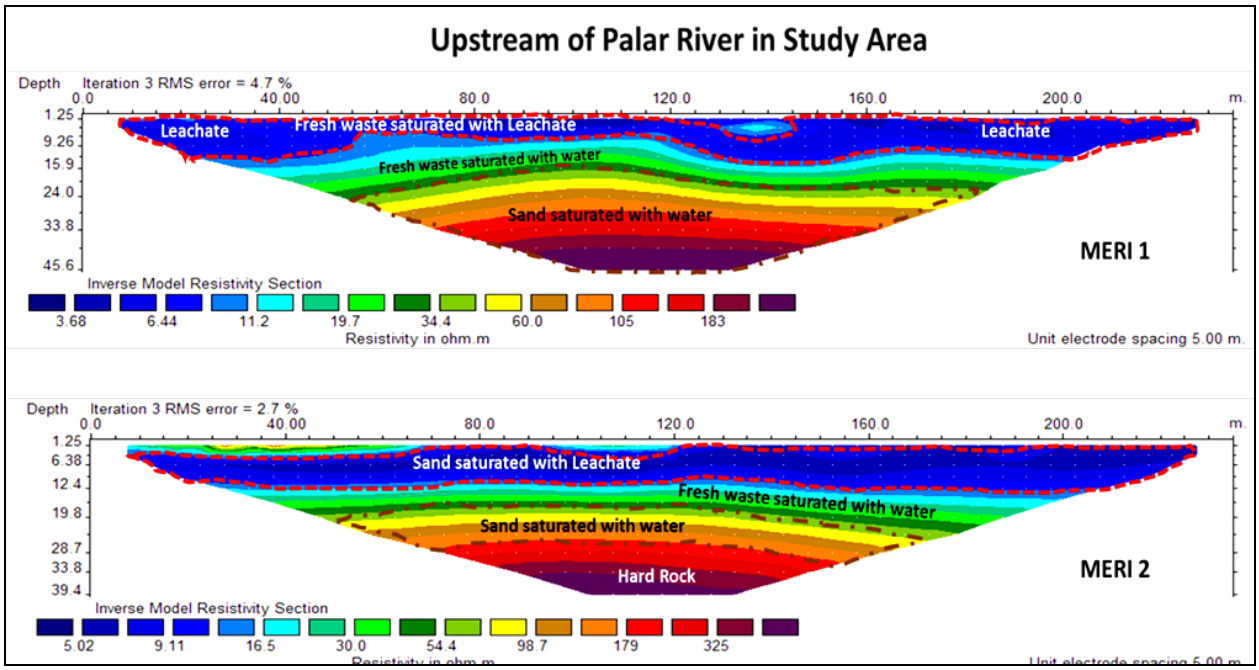


**Fig 6a:** Upstream of Palar River in Study area

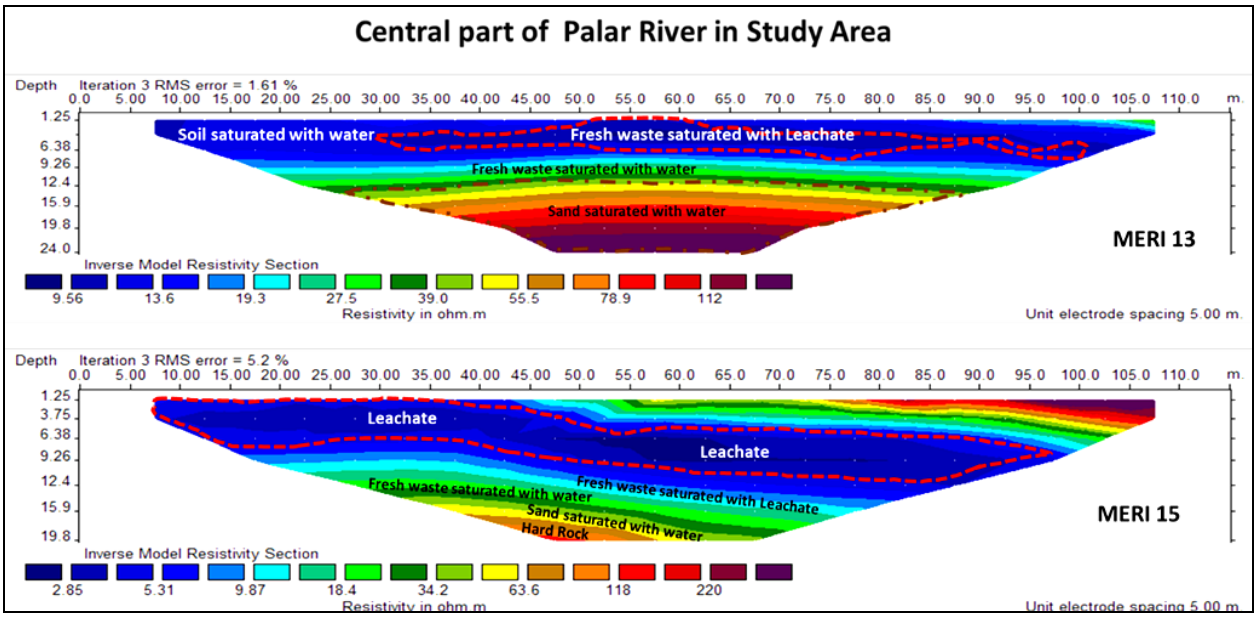


**Fig 6b:** Central Part of Palar River in Study area

**Table 2:** Electrical Resistivity of Earth Materials *

| Sampled Material | Resistivity (Ωm) |
|---|---|
| Leachate only | 2.994 |
| Sand saturated with leachate | 4.97-5.04 |
| Fresh waste (plant materials, rubber strands, sand) saturated with leachate | 6.03-7.16 |
| Soil saturated with leachate | 3.15-4.00 |
| Rain water only | 73.88 |
| Sand saturated with rain water | 14.36-1750 |
| Fresh waste (plant materials. rubber strands, sand) saturated with rain water | 19.71-22.50 |
| Soil saturated with rainwater | 9.30-10.57 |
| Clay saturated with brackish water | 0.12-0.20 |
| Clean sand saturated with sea water | 1.5-3.5 |
| Fresh sandstone | 600 |
| Phyllite | 300 |
| Hard rock | >600 |

* After (Shaharin, 1998).

**Table 3:** Inferred degree of contamination for MERI profile

| Profiles | Depth | Resistivity (Ωm) | Rate of Contamination |
|---|---|---|---|
| MERI 1 | 0-1.25 | <3.68 | Highly Contaminated |
| | 1.25-15.9 | 3.68-6.44 | Moderately Contaminated |
| | 15.9-24 | 6.44-34.4 | Less Contaminated |
| | >24 | 34.4-above 183 | Not Contaminated |
| MERI 2 | 0-1.25 | <5.02 | Moderately Contaminated |
| | 1.25-12.4 | 5.02-9.11 | Less Contaminated |
| | >12.4 | 9.11-above 325 | Not Contaminated |
| MERI 13 | 0-1.25 | <9.56 | Moderately Contaminated |
| | 1.25-9.26 | 9.56-19.3 | Less Contaminated |
| | >9.26 | 19.3-above 112 | Not Contaminated |
| MERI 15 | 0-12.4 | <2.85 | Extremely Contaminated |
| | 12.4-15.9 | 2.85-18.4 | Moderately Contaminated |
| | >15.9 | 18.4-above 220 | Not Contaminated |
| MERI 26 | 0-3.75 | 94.5-165 | Not Contaminated |
| | 3.75-12.4 | 3.29-5.75 | Extremely Contaminated |
| | >12.4 | 5.75-165 | Less Contaminated |
| MERI 23 | 0-1.25 | 4.63-8.67 | Less Contaminated |
| | 3.75-12.4 | 2.48-3.39 | Extremely Contaminated |
| | 12.4-15.9 | 3.39-6.34 | Highly Contaminated |
| | >19.8 | 6.34-above 22.2 | Not Contaminated |

Aquifer vulnerability index in the study area shows that the degree of contamination decreases with depth along the three profiles and that soil and aquifers of the study area are vulnerable to contamination at shallow levels. Since we interpreted the topsoil as being Sandy soils with less clayey content, effluent infiltration in the study area is enhanced by the lack of protective layers as shown by the correlation between longitudinal conductance and over burden protective capacity. Based on the VES interpretation the longitudinal conductance was evaluated and it was observed that maximum area falls in the good protective Capacity and Moderate Vulnerability and few are falling in Moderate protective Capacity and High Vulnerability (Table 4). The topsoil in the entire study area is porous and permeable and is therefore conducts for effluent discharged. Hence, the soils and groundwater resources around the river course might be polluted by the Effluent. We imagine that with time the contamination may contribute to pollution of the ground water and this is of great threat to farming and future exploitation of underground water resources in the area. This work shows that contamination is not limited to in and around palar river. To avoid further pollution of the soil and groundwater aquifers in the study area, we recommend to stop indiscriminate Effluent Discharge practices.

**Table 4:** Standard values for longitudinal conductance/protective capacity rating and classification of Aquifer Vulnerability on the basis of hydraulic resistance

| Si (mho) | Protective capacity Rating [30] | Log (Hydraulic Resistance) in Years | Vulnerability [26] |
|---|---|---|---|
| >10 | Excellent | >4 | Extremely Low Vulnerability |
| 5-10 | Very Good | 3-4 | Low Vulnerability |
| 0.7-4.9 | Good | 2-3 | Moderate Vulnerability |
| 0.2-0.69 | Moderate | 1-2 | High Vulnerability |
| <0.1-0.19 | Poor-week | <1 | Extremely High Vulnerability |

## Conclusion

The study area is characterized dominantly by Topsoil, sandy, clayey sand and then followed by hard strata. The low resistivity is observed close to the river course. The results from electrical sounding show the HA type curves which is correlated positively with those of 2D images as zones of contamination are characterized by very low resistivity values relative to the background resistivity of rocks. The Effluent is interpreted as a flow anomaly on the 2D image profiles with the maximum depth of infiltration at about 15 m. The correlation between longitudinal conductance and overburden protective capacity show that aquifer in the study area have moderate to good protective capacity and moderate to highly vulnerable to contamination. Clayey geoelectric layers in the study area are located farther from the aquifer zone.

## Acknowledgement

This study is the research topic of the author carried out during perusing his Ph.D. in Osmania University, Hyderabad, India. The authors express their gratitude to the respective farmers and well owners for providing valuable information during well inventory and field investigations.

## References

1. Fisher H and Pearce D. Salinity reduction in tannery effluents in India and Australia. ACIAR Impact assessment series Report No. 61, 2009, 1-56.
2. Gonzalez-Macias C, Schifter I, Luich-Cota DB, Mendez Rodriguez, L. and Hernandez-Vazquez, S. Distribution, enrichment and accumulation of heavy metals in coastal sediment of salina Cruz bay, Mexico. Environmental Monitoring and Assessment, 2006, 211-230. DOI: 10.1007/s10661-006-1492-8.
3. Bhaskaran TR. Treatment and disposal of tannery effluents. Central Leather Research Institute (CLRI), Madras, 1977.
4. Stampolidis A, Tsourlos P, Soupios P, Mimides TH, Tsokas G, Vargemezis G and Vafidis A. Integrated geophysical investigation around the brackish spring of

Rina, Kalimnos Isl., SW Greece. Jour. Balk Geophys. Soc. 2005; 8(3):63-73.
5. Kalisperi D, Soupios P, Kouli M, Barsukov P, Kershaw S, Collins P and Vallianatos F Coastal aquifer assessment using geophysical methods (TEM, VES), case study: Northern Crete, Greece. In: 3rd IASME/WSEAS international conference on geology and seismology (GES '09) Cambridge, UK, 2009, 24-26.
6. Zohdy A, Eaton GP and Mabey DR. Application of surface geophysics to ground-water investigations: techniques of water resources investigations of the United States Geological Survey, chap D1, book 2, 116 p, 1974.
7. Soupios P, Kouli M, Vallianatos F, Vafidis A and Stavroulakis G. Estimation of aquifer parameters from surficial geophysical methods. A case study of Keritis Basin in Crete. Jour. Hydrol., 2007; 338:122-131.
8. Shankar KR. Affordable water supply and sanitation. In: Groundwater exploration 20th WEDC Conference Colombo, Sri Lanka, 1994, 225-228.
9. Lashkaripour GR. An investigation of groundwater condition by geoelectrical resistivity method: a case study in Korin aquifer, southeast Iran. Jour. Spatial Hydrology, 2003; 3:1-5.
10. Oseji JO, Asokhia MB and Okolie EC. Determination of groundwater potential in Obiaruku and environs using surface geoelectric sounding. Environmentalist. 2006; 26:301 308.
11. Sahu PC and Sahoo H. Targeting groundwater in tribal dominated Bonai area of drought-prone Sundargarh District, Orissa, India. A combined geophysical and remote sensing approach. Jour. Hum. Ecol. 2006; 20:109-115.
12. Palacky GJ. Clay mapping using electromagnetic methods. First Break. 1987; 5:295-306.
13. Zohdy AAR and Martin RJ. A study of seawater intrusion using direct-current soundings in the southern part of the Oxward Plain, California. Open-File Report, USGS. 1993; 139:93-524.
14. Choudhury K and Saha DK. Integrated geophysical and chemical study of saline water intrusion. Ground Water. 2004; 42:671-677.
15. Sankaran S, Rangarajan R, Krishna Kumar K, Saheb Rao S and Smitha H. Geophysical and tracer studies to detect subsurface chromium contamination and suitable site for waste disposal in Ranipet, Vellore district, Tamil Nadu, India. Environ. Earth Sci., 2010a; 60(4):757-764.
16. UNDP (United Nations Development Programme). Groundwater investigations in Tamil Nadu. Technical Report prepared for Government of India by the United Nations, New York, 1971, 1-87.
17. Gupta CP, Thangarajan M, Rao VVSG, Ramachandra YM and Sarma MRK. Preliminary study of groundwater pollution in the Upper Palar basin and feasibility of mass transport modeling to predict pollutant migration. NGRI Tech Rep. No. 94-GW-168, 1994.
18. Koefoed O. Resistivity sounding measurements. In: Geosounding Principles. Elsevier, New York, 1979, 1.
19. Griffiths DH, Turnbull J and Olayinka AI. Two-dimensional resistivity mapping with a computer-controlled array. First Break. 1990; 8:121-129.
20. Griffiths DH and Barker RD. Two-dimensional imaging modelling in areas of complex geology. Jour. Appld. Geophys. 1993; 20:211-226.
21. Owen RJ, Gwavava O and Gwaze P. Multi-electrode resistivity survey for groundwater exploration in the Harare greenstone belt, Zimbabwe. Hydrogeological Jour. 2005; 14:244-252.
22. Schlumberger C. Etude sur la Prospection Electrique du Sous-sol, Gaultier-Villars et Cie. Paris, 1920, 94.
23. Bhattacharya PK and Patra HP. Direct current geoelectrical sounding, principles and interpretation. Elsevier, Amsterdam, 1968: 135p, 1920.
24. Orellana E and Mooney HM. Master tables and curves for vertical electrical sounding over layered structures. Interciencia, Costanilla de los Angles, 15, Madrid, 1966.
25. Van Der Velpen BPA. A computer processing package for D.C. resistivity interpretation for an IBM compatible. ITC Jour., v.4, The Netherlands, 1988.
26. Van Stempvoort D, Ewert L, Wassenaar L Aquifer vulnera bility index: a GIS-compatible method for groundwater vulner ability mapping. Can Water Resour J, 1992, 18:25-37
27. Kirsch R. Groundwater protection: vulnerability of aquifers. In: Kirsh R (ed) Groundwater geophysics a tool for hydrogeology. Springer, Berlin, Heidelberg, 2006, 468-480
28. Freeze RA, Cherry JA. Groundwater. Prentice Hall, New Jersey, 1979.
29. Henriet JP Direct application of the Dar Zarrouk parameters in groundwater surveys. Geophys Prospect. 1976; 24:344-353
30. Oladapo MI, Mohammed MZ, Adeoye OO, Adetola BA. Geoelectrical investigation of the Ondo State Housing Corpora tion Estate, Ijapo Akure, Southwestern Nigeria. J Min Geol. 2004; 40(1):41-48
31. DEY, A. and MORRISON, H.F. Resistivity modelling for arbitrary shaped two-dimensional structures. Geophysical Prospecting. 1979; 27:106-136.
32. Loke MH and Barker RD. Rapid least squares inversion of apparent resistivity pseudosections by a quasi-Newton method. Geophysical Prospecting, 1996; 44:131-152.
33. Rosqvist H, Dahlin T, Fourie A, Rohrs L, Bengtsson A, Larsson M Mapping of leachate plumes at two landfill sites in South Africa using geoelectrical imaging techniques. In: Proceedings of the 9th international waste management and landfill sympo sium, Cagliari, Italy, 2003, 1-10.
34. Hamzah U, Mark J, Nur Atikah MA. Electrical resistivity techniques and chemical analysis in the study of leachate migration at Sungai Sedu Landfill. *Asian J Appl Sci*, 2014; 7:518-535
35. Ariyo SO, Omosanya KO, Oshinloye BA. Electrical resistivity imaging of contaminant zone at Sotubo dumpsite along Sagamu Ikorodu Road, Southwestern Nigeria. Afr J Environ Sci Technol, 2013; 7:312-320
36. Shaharin, I. Investigation and Assessment of Municipal Landfill Sites in the Federal Territory of Kuala Lumpur (unpublished report), 1998.